JOURNAL OF Applied Polymer SCIENCE

A Design of Composite Hollow Fiber Membranes with Tunable Performance and Reinforced Mechanical Strength

Rui-Xin Zhang,[1] Tianyin Liu,[2] Leen Braeken,[3] Zaihao Liu,[2] Xiao-Lin Wang,[2] Bart Van der Bruggen[1]

[1]Department of Chemical Engineering, KU Leuven, B-3001 Leuven, Belgium

[2]Department of Chemical Engineering, State Key Laboratory of Chemical Engineering, Tsinghua University, Beijing 100084, China

[3]Department of Industrial Sciences, Lab4U, KH Limburg, B-3590 Diepenbeek, Belgium

Correspondence to: R.-X. Zhang (E-mail: ruixin.zhang@cit.kuleuven.be)

ABSTRACT: A new design of hollow fiber membranes with high mechanical strength, great surface area per volume ratio and tunable filtration performance is presented. This newly developed hollow fiber membrane was produced by an intensified production process, in which the processes of thermally induced phase separation (TIPS), non-solvent induced phase separation (NIPS), and interfacial polymerization (IP) were combined. PVDF (polyvinylidene difluoride) hollow fiber membranes (produced by TIPS) were used as support substrates. Afterwards, PES (polyethersulfone) (made by NIPS) and PA (polyamide) layers (manufactured by IP) were coated one by one. The pure water permeability, molecular weight cut off (MWCO), salt rejection, tensile stress together with surface and cross-sectional morphology indicate that the properties of the hollow fiber membranes can be easily adjusted from microfiltration-like to nanofiltration-like membranes only by varying the presence of the IP step and the concentration in the PES layer in the production system. © 2014 Wiley Periodicals, Inc. J. Appl. Polym. Sci. **2015**, *132*, 41247.

KEYWORDS: membranes; separation techniques; synthesis and processing

Received 21 October 2013; accepted 29 June 2014
DOI: 10.1002/app.41247

INTRODUCTION

As a possible solution to support sustainable industrial growth, process intensification has gained more attention. According to this concept, manufacturing and process design requires substantially decreasing equipment volume, energy consumption and waste formation, ultimately leading to smaller, cheaper, safer, cleaner, more compact, and sustainable technologies.[1–3] Following this strategy, a proper design of a compact membrane manufacturing process, producing membranes with tunable performance from microfiltration to nanofiltration, is of great interest.

Membrane processes, with its advantages of a relatively small footprint, easy operation and, in some cases, lower energy consumption, have many applications in separation and purification.[4] Comparing with disinfection, distillation, or media filtration, pressure-driven membrane processes remain the most favourable technologies for water treatment, since no chemical additives, thermal inputs, or regeneration of spent media are required in the system.[5] According to characteristic pore size or intended applications, pressure-driven membranes are typically classified into microfiltration (MF), ultrafiltration (UF), nanofiltration (NF), and reverse osmosis (RO). Characteristic pore sizes of MF membranes generally range from 0.05 μm to 10 μm, typically between 0.1 μm and 0.8 μm.[6] UF characteristic pore sizes vary between 0.005 μm and 0.15 μm, typically from 0.01 μm to 0.05 μm (300 to 300,000 Daltons).[6] Accordingly, for removal of most suspended solids, colloids, protozoa, bacteria, fungus cysts and some viruses, MF performs well, while, UF can reject all the other viruses, colloids and pathogens.[5,6] Regarding low molecular weight organic matter and ionic species, NF and RO is considered the best choice.[5,6]

These membrane types can be implemented by several membrane configurations, such as flat-sheet (e.g., plate-and-frame and spiral wound modules), tubular and hollow fibers. Among these configurations, hollow fibers have been considered to be an attractive alternative for various membrane applications because of (1) its high productivity per unit volume of membrane module (i.e., enormous membrane surface area per unit shell volume and high packing density);[6–9] (2) self-supporting;[7–9] and (3) good flexibility in operation.[7,9] Typically, the ratio of surface area to volume (m^2/m^3) for plate-and-frame modules is 350 to 500, and the ratio for spiral wound modules is 650 to 800. However, for hollow fiber modules, the ratio is as high as 7000 to 13,000.[10] Additionally, unlike the complex fabrication with spacers and/or porous supporters for flat-sheet membrane modules, the self-supporting property of hollow fiber membranes greatly simplifies the manufacturing process.[10]

Among the methods for preparation of hollow fiber membranes, phase inversion, including thermally induced phase separation (TIPS) and immersion precipitation or non-solvent induced phase separation (NIPS), are widely used.[3,11] As a main approach for preparation of MF hollow fiber membranes, TIPS is achieved by cooling down the polymer solution. Once the polymer rich phase is solidified, the porous membrane structure can be created by extracting the solvent from the polymer poor phase.[12] Conventional TIPS methods tend to produce isotropic (dense or porous) membrane structures with high mechanical strength and narrow pore size distribution.[3,6] However, the pore size cannot be further reduced to nano-scale, which limits the applicability of this method. In contrast to the isotropic structures produced by TIPS, NIPS creates an asymmetric porous structure with a dense skin at the outer surface. This structure is induced by exchange of solvent in polymer solution with non-solvent in a coagulation bath.[13] Due to the dense surface structure, the pore size of the hollow fiber membranes prepared by NIPS method can be reduced to dozens of nanometers. Whereas, if NF or RO is required, typically, a porous hollow fiber substrate made by NIPS should be deposited by an ultrathin selective layer fabricated by interfacial polymerization (IP). Although the NIPS process together with the IP approach (NIPS-IP) provides great flexibility to tailor the membrane structure and properties, the macrovoids presented in the hollow fiber porous matrix bring a serious drawback.[6] The macrovoids exhibit through the entire cross section of the fiber matrix leading to lower the elongation and the tensile strength, and thus decreasing the rigidity of the fiber and limiting its ability to withstand hydraulic pressures.[6,8]

In order to overcome these limitations (i.e., mechanical strength and tunable performance), a proper design of a compact membrane manufacturing process, producing membranes with tunable performance from microfiltration to nanofiltration, is of great interest. Some researchers adapted the manufacturing method from flat sheet membrane to have a tubular braid as a support of the membrane and coated the polymer film on it.[14–16] The braids used for supporting are typically of a relatively large diameter (>15 mm).[15] Although the mechanical strength of these braid reinforced hollow fiber membranes has been greatly improved, the surface area to volume ratios of the membrane module is reduced because of the large diameters of the supporting braids. Consequently, fewer fibers or less surface area per membrane unit result in less filtration efficiency. In addition to this large diameter, another problem encountered with the braid reinforced hollow fiber membranes is the filtration reliability.[14] When a larger pore size of a membrane is needed (e.g., MF), for instance, the concentration of the polymer casting solution should be decreased. The diluted polymer solution leads to penetration through the braid, and large voids formed in the cross section. These functions may result in defects formed on the membrane surfaces, which deteriorate the filtration performance.

In this work, a new design of hollow fiber membranes is presented, which may overcome all the limitations of the aforementioned membranes and maintain not only a high mechanical strength and filtration reliability, but also provide a great surface area per volume ratio and tunable filtration performance. This newly developed hollow fiber membrane is manufactured by an intensified production process, in which the TIPS, NIPS, and IP methods are combined. In this intensified process, PVDF hollow fiber membranes made by TIPS method are produced first and serve as porous and rigid supporting matrixes. Afterwards, NIPS (polyethersulfone, PES) and IP (polyamide, PA) processes are followed one by one. The influence of the concentration of polyethersulfone polymer solution and the employment of the IP step will be studied. The transformation in the structures and properties (i.e., filtration performance, MWCO, mean pore size and tensile stress at break) of the new designed hollow fiber membranes will be evaluated.

MATERIALS AND METHODS

Materials

Shell-feeding Microza PVDF hollow fiber microporous membranes produced by TIPS method were supplied by Asahi Kasei (Japan) and used as supporting matrixes. The internal and external diameters of the PVDF hollow fibers were 0.8 mm and 1.2 mm, respectively. The average pore diameter was 150 nm and the porosity was 70%. Polyethersulfone (PES) powder (Veradel 3000P) was provided by Solvay Advanced Polymer (Belgium). N-methyl pyrrolidone (NMP, >98%) and hexane (>97%) were obtained from Sinopharm Chemical Reagent China Co., Ltd. M-phenylenediamine (MPD, >99%) and trimesoylchloride (TMC, >99%) used for synthesizing polyamide thin films were supplied by J&K Scientific Beijing Co., Ltd. (China). Anhydrous sodium sulphate (Na_2SO_4, >99%) was purchased from Beijing Modern Eastern Fine Chemical Co., Ltd. Dextran (20 kDa, 40 kDa, and 100 kDa) and PEO (200 kDa) were obtained from Acros Organics. All the chemicals were used as received without further purification.

Preparation of Composite Hollow Fiber Membranes with PVDF Hollow Fibers as Supporting Matrix

In the first step of the production process, a hollow fiber matrix was prepared by thermally induced phase separation (TIPS). Afterwards, a polymer film produced by non-solvent induced phase separation (NIPS) was coated on the surface of this hollow fiber matrix. In this study, a commercial shell-feeding PVDF hollow fiber matrix with water permeability of 1500 L m^{-2} h^{-1} bar^{-1} was directly used for convenience. This PVDF matrix was further coated by a PES film. The preparation details of the PES coating are similar with the protocol as described in our previous work.[13] Briefly, the mixture of PES powder and NMP was agitated until homogeneous in airtight glass bottles. Air bubbles were removed before coating. The PVDF support membrane was rotated and coated with a thin layer of PES solution in an ambient condition and directly immersed in a de-ionized water bath. After 2 h, the PVDF-PES membrane was thoroughly washed with de-ionized water and dried by compressed air for 10 min. Four pieces of PVDF-PES hollow fiber membranes were potted into a transparent polyurethane tube with an inner diameter of 6 mm and an effective length of 15 cm. The membrane module was sealed by epoxy.

If a NF or RO membrane was needed, the process was followed by an interfacial polymerization (IP) step. This step is to produce a polyamide (PA) thin film over a PVDF-PES membrane. In the

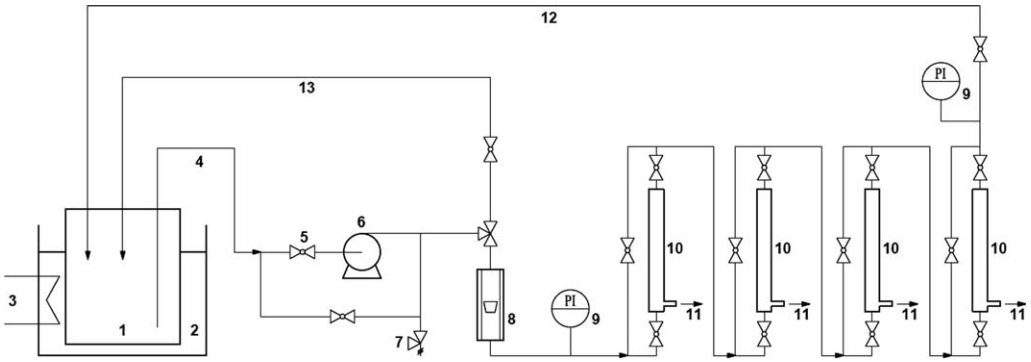

Figure 1. Schematic representation of the filtration system. (1) Feed vessel; (2) constant temperature water bath; (3) heat exchanger; (4) feed line; (5) ball valve; (6) booster pump; (7) pressure relief; (8) flow meter; (9) pressure indicator; (10) membrane modules; (11) permeate line; (12) retentate line; (13) bypass line.

PVDF-PES membrane module, the shell sides of the membranes were immersed in a 2 w/v % aqueous solution of MPD for 1 h. The excess MPD solution was removed by harsh flushing of Argon gas. The membranes were then saturated with a TMC organic solution. After 10 min contact, the solution was drained. The final PVDF-PES-PA membranes were washed by hexane (3 min) and de-ionized water (10 min) in turn in order to remove unreacted monomer in the membrane module.

For the purpose of understanding the properties of this new designed hollow fiber membrane and investigating the transformational properties of both PVDF-PES and PVDF-PES-PA membrane configurations, the concentration of the PES coating solution for PVDF-PES configuration was verified from 13 w/v % to 34 w/v %, and the concentration of the transitional PES layers for PVDF-PES-PA configuration ranged from 13 w/v % to 28 w/v %. The interval of the PES concentration is 3 w/v % in all cases.

Membrane Performance Evaluation

In order to determine the filtration performance (i.e., pure water permeability, solute seperation), a filtration system was designed as shown in Figure 1. Each membrane module consisted of four certain types of hollow fiber membranes with an effective length of 12 cm and effective membrane area of around 5.3 cm^2. The ends of the fibers were glued with silicon pad and then potted into a tubular stainless steel shell. The shell and the silicon pad were sealed by a clamp so as to stand the operational pressure. The membrane compaction was carried out at 4 bar for 2 h prior to each measurement. A relatively high cross flow velocity of the feed solution (1 L min^{-1}) was applied in order to minimize the effect of concentration polarization. The pressure was set at 4 bar for all cases. The temperature was controlled at 25 ± 0.2°C by a heat exchanger.

The measurement of pure water permeability (A) was carried out by filtering de-ionized water and calculated by dividing the pure water flux (J_w) by the transmembrane pressure (ΔP), $A = J_w/\Delta P$.

The solute separation of the membranes (dextran, PEO or Na_2SO_4) was calculated by eq. (1):

$$R(\%) = (1 - c_p/c_c) \times 100 \quad (1)$$

where c_p and c_c refer to solute concentrations in permeate and concentrated streams, respectively. The feed concentrations were 1000 ppm for Na_2SO_4 solution, and 1500 ppm for dextran (molecular weight of 20 kDa, 40 kDa, and 100 kDa) and PEO (molecular weight of 200 kDa) solutions. The concentration of Na_2SO_4 was determined by conductivity, and the concentration of neutral organic compounds were analysed by a total organic carbon analyser (TOC-V_{CPN}; Shimadzu, Japan). The average values of twelve hollow fiber membranes in three modules were evaluated in all cases.

Membrane Characterization

Field Emission Scanning Electron Microscope and Tensile Strength Analysis. The outer surface morphologies of the hollow fiber membranes were characterized by a field emission scanning electron microscope (FESEM, 6301F, JEOL). The cross-sectional morphologies were measured by a scanning electron microscopy (SEM), using a Philips XL30 FEG SEM (Eindhoven, The Netherlands). The dry membrane was immersed in liquid nitrogen for around 1 min. The frozen fragments of the membrane were broken and taped on a holder with carbon glue. The samples were sputtered with gold at 10 mA for 5 min and vacuumed for 1 h before the measurement. The accelerating voltage was set at 15 kV. Tensile strength test of the hollow fiber membranes was measured using a Table-top Type Universal Tester (AGS-J), Shimadzu Co. Ltd. The average values of twelve hollow fiber membranes are reported.

Pore Size Characterization. The pore size of the membranes is represented by the retention properties. The Stokes diameter (d_s) is reported to have a good correlation with retention for UF membranes.[17,18] The Stokes radius (hydrodynamic radius) is the radius of a hypothetical rigid sphere that diffuses at the same rate as the molecule under study.[19–21] Hydration and shape effects of this sphere are considered. It can be calculated using the Stokes-Einstein equation as described by Singh et al.[21] The Stokes radii of dextran and PEO, r_s (Å), with a function of molecular weight (M_w) are given by[22,23]

$$r_s(\text{dextran}) = (0.096 \times M_w^{0.59} + 0.128 \times M_w^{0.5})/2 \quad (2)$$

$$r_s(\text{PEO}) = 2.088 \times 10^{-3} \times M_w^{0.587} \quad (3)$$

The Stokes diameter is defined as[17,20]

$$d_s = 2r_s \quad (4)$$

Table I. Pure Water Permeability (PWP), Porosity, Tensile Strength at Break and Strain at Break of PVDF-PES Hollow Fiber Membranes Manufactured by Different Concentrations of PES Coating Solutions with the Same PVDF Hollow Fiber Substrates

Concentration of PES (%)	PWP (L m^{-2} h^{-1} bar^{-1})	Porosity (%)	Tensile strength at break (MPa)	Strain at break (%)
0	1500.00 ± 10.00	76.0 ± 1.98	11.65 ± 0.24	125.80 ± 2.39
13	1417.97 ± 27.13	74.8 ± 1.07	11.64 ± 0.40	65.37 ± 1.96
16	513.76 ± 27.15	73.3 ± 0.98	12.94 ± 0.39	60.28 ± 1.50
19	84.87 ± 19.50	71.2 ± 1.20	15.62 ± 0.25	64.82 ± 1.37
22	24.22 ± 3.59	70.2 ± 0.74	17.26 ± 0.52	68.81 ± 2.24
25	16.16 ± 4.60	69.4 ± 1.01	17.35 ± 0.62	52.44 ± 1.84
28	1.16 ± 0.29	67.1 ± 1.27	20.16 ± 0.59	49.70 ± 1.24

In this work, the retention versus molecular weight (M_W) of organic solutes was plotted to determine the mean pore size and molecular weight cut-off (MWCO). The mean pore size of the membranes was represented by the d_s corresponding to 50% retention.[20] The M_W of the solute with a retention of 90% determined the MWCO of each membrane.[17,20] The standard deviations of the mean pore size and the MWCO were below 5%.

RESULTS AND DISCUSSION

From Microfiltration (MF) to Ultrafiltration (UF)

Pure Water Permeability (PWP). The PVDF hollow fiber substrates were coated by different concentrations of PES solutions. The pure water permeability (PWP) of these hollow fiber membranes is listed in Table I. The results show that the PWP of PVDF-PES hollow fiber membrane is significantly influenced by the concentration of the PES coating. The neat PVDF hollow fiber membrane has a PWP of 1500 L m^{-2} h^{-1} bar^{-1}. An additional PES layer with concentration of 13% reduces the PWP to 1418 L m^{-2} h^{-1} bar^{-1}, which is slightly lower than the one for the neat PVDF membrane. However, further increasing the concentrations of the PES coating solutions from 13% to 22%, the PWP significantly reduces from 1418 to 24.22 L m^{-2} h^{-1} bar^{-1}. When the concentrations of PES vary from 25 to 28%, the PWP continually reduces from 16.16 to 1.16 L m^{-2} h^{-1} bar^{-1}. The PWP of the membranes with 31 and 34% of PES is 0.072 and 0.019 L m^{-2} h^{-1} bar^{-1}, respectively. Apparently, the higher concentrations lead to higher viscosity of the polymer solutions, which result in the smaller pore size, the higher density of the PES layers. These changes of the membrane structures lead to the higher membrane resistance.

Characterization of PVDF-PES Hollow Fiber Membranes. The organic solute retention versus molecular weight for the PVDF-PES hollow fiber membranes manufactured using different concentrations of PES coating solutions is presented in Figure 2. The neat PVDF substrate and the membrane manufactured with 13% of PES coating solution did not reject any of the solutes used in the test. Considering the ultra low flux of the membranes manufactured with 31 and 34% of PES solutions, the retentions of these membranes were not tested here. It is observed that by further increasing the concentration of the PES layers, the retention increases for all compounds. Comparing the retentions of the same solute, generally, the membranes coated with higher concentrations of PES solutions exhibit higher retentions, which indicate that the pore size becomes smaller.

The value of mean pore size and MWCO as shown in Table II are calculated from the organic solute separation curves (Figure 2). From Table II, it can be seen that, these membranes have similar MWCO. However, the values of the mean pore sizes vary greatly. As shown in Figure 2, the PVDF-PES membrane coated by 16% of PES rejected less than 20% of dextran with M_w of 100 kDa, but the membrane with 28% of PES has a rejection of around 75%. Similar to this rejection performance, the membranes coated by higher concentrations of PES exhibit higher rejections of the low molecular dextran (<190 kDa). This indicates the membranes coated by higher concentrations of PES have a larger portion of small pores that can reject the dextran smaller than the MWCO.

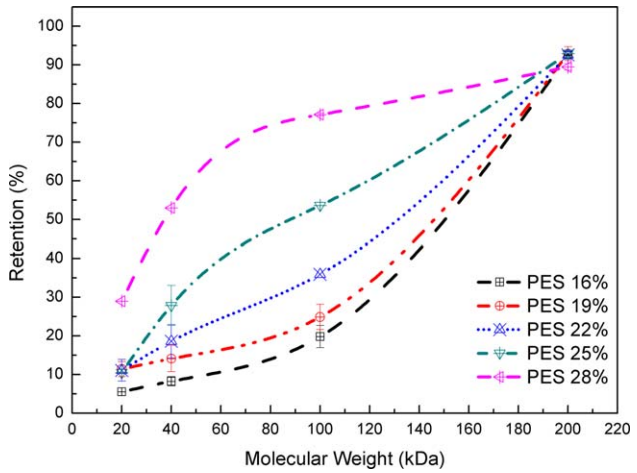

Figure 2. Organic solute separation curves for PVDF-PES hollow fiber membranes manufactured by different concentrations of PES coating solutions with the same PVDF hollow fiber substrates. The organic solutions filtrated in the study were 1500 ppm of dextran (molecular weight of 20 kDa, 40 kDa and 100 kDa) and of PEO (molecular weight of 200 kDa) solutions. [Color figure can be viewed in the online issue, which is available at wileyonlinelibrary.com.]

Table II. Mean Pore Size and Molecular Weight Cut off of PVDF-PES Hollow Fiber Membranes Manufactured by Different Concentrations of PES Coating Solutions with the Same PVDF Hollow Fiber Substrates (Calculated from the Organic Solute Separation Curves)

Concentration of PES (%)	16	19	22	25	28
Mean pore size[a] (nm)	15.5	15.2	14.4	11.9	7.1
Approx. molecular weight cut off, (kDa)	196.5	195.9	195.5	192.4	200

[a] Calculated from eqs. (2) and (4).

The porosity of these membranes is also tested and listed in Table I. The additional PES coating makes the membranes less porous. After coating a PES layer, the porosity of the membranes gradually decreases from around 76 to 67%. This less porous structure together with the small pore size of the PVDF-PES membranes results in a high transport resistance, which explains the decrease in PWP.

The mean pore size of the neat PVDF MF hollow fiber membranes is around 150 nm and they cannot reject the organic solute with M_w of 300 kDa. After coating the PES layers, the mean pore size of the membranes is reduced to around 10 nanometers and the MWCO decreases to around 200 kDa. These changes indicate that the coating of the PES layers can successfully change the performance of membranes from microfiltration to ultrafiltration.

Besides the separation performance, the mechanical strength (represented by the tensile strength and strain at break) is another important characteristic of hollow fiber membranes, as a good rigidity of fibers allows withstanding high hydraulic pressures and further assures the performance and lifespan of membranes. Generally, the tensile strength at break for PES hollow fiber membranes made by NIPS (without support) is around 4 to 5 MPa, which is significantly lower than the ones made by TIPS. The neat PVDF membrane (TIPS) used in this study has a tensile strength at break of 11.65 MPa and a strain of 125.8%. As shown in Table I, when the concentration of the PES layer increases, generally, the tensile stress at break greatly increases and the strain at break decreases. Although the tensile strength for the membrane with 13% of PES layer is similar as the neat PVDF membrane, the tensile strength at break can reach up to 20.16 MPa (28% of PES) by further increasing the concentration of PES. This value is significantly larger than the ones for the normal PES or PVDF hollow fiber membranes. The strain at break of the membranes can be reduced from around 126% to around 50% by adding a PES layer. This low strain at break indicates that the membrane with a PES layer has less structure change than the neat PVDF membrane under the same hydraulic pressure.

This good mechanical strength together with the tunable separation performance suggests that the combination of the TIPS and NIPS methods to produce hollow fiber membranes not only provides a great flexibility to tailor the membrane performance for separation purposes (from microfiltration to ultrafiltration), but also yields a high rigidity of hollow fiber membranes.

Surface and Cross-Sectional Morphologies of PVDF-PES Hollow Fiber Membranes. The cross-sectional morphologies of PVDF-PES hollow fiber membranes with different concentrations of PES coating layers are shown in Figure 3. The morphologies and structures of the PES layers are affected by the concentrations of the coating solution. As shown in Figure 3, the shape of the macrovoids changes from circular to a finger-like structure. As the concentration of the PES coating solution increases, the macrovoids decrease in size and the thickness of the entire PES layer increases. These changes in structures are caused by the different viscosity of the PES polymer solution and the delayed demixing process. When the concentration increases, the PES coating solution becomes more viscous, which results in a thicker PES layer adhered on the membrane surface. Additionally, as Kools[24] reported, when increasing the concentration of the polymer solution, the demixing of the membrane forming system is delayed. The delay time detected by light transmission experiments in the membrane system increases with increasing the polymer concentration. Due to this delayed demixing, a denser and more uniform surface was formed as the PES concentration increases, which can be observed in Figure 3. This dense and uniform structure explains the better rejection and the lower mean pore size of the membrane with a higher concentration of PES. The gradually changed structures also explain the tunable filtration performance discussed above. For the membranes with higher concentration of PES layers, the thicker PES layer, smaller finger-like macrovoids together with the dense surface generate higher transport resistance to the pure water permeation and higher resistance to the tensile stress. The structure along with the performance of the membranes indicates that the PVDF hollow fiber MF membranes can be successfully transferred to UF membranes with tunable filtration performance by simply adjusting the concentrations of the PES layers.

From Ultrafiltration (UF) to Nanofiltration (NF)

Surface Morphology of PVDF-PES-PA Hollow Fiber Membranes. When further coated by a polyamide (PA) layer, the surface morphology of the PVDF-PES hollow fiber membrane is changed from flat surface to a ridge-and-valley structure as reported by others (Figure 4).[25–27] When the two monomers (i.e., MPD in the aqueous phase and TMC in the organic phase) are brought into contact, the interfacial polymerization predominantly occurs by the diffusion of diamines from the aqueous phase into the organic phase, which is caused by the greater solubility of MPD in the organic phase compared to the TMC solubility in water.[28,29] This polyamide thin film on top of the porous support is responsible for the high salt rejection and water flux properties of the thin film composite membrane. From the morphologies shown in Figure 4, it is obvious that the properties of the support layer influence the polyamide morphology. The ridge-and-valley structures of the polyamide

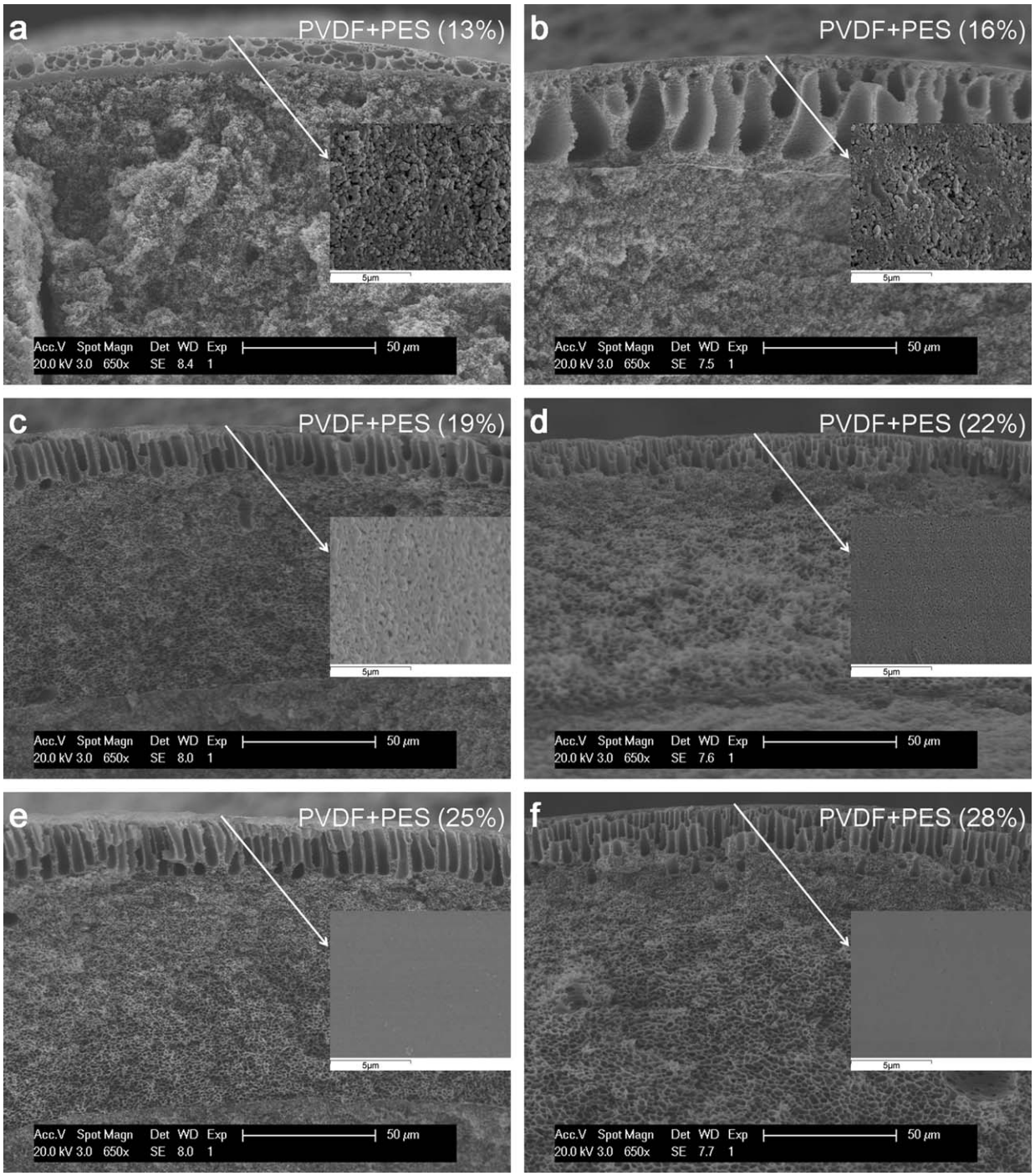

Figure 3. Surface and cross section morphologies of PVDF-PES hollow fiber membranes manufactured by different concentrations of PES coating solutions with the same PVDF hollow fiber substrates.

become regular and dense when increasing the concentrations of the support PES layers. This difference in polyamide layer surface morphology is caused by the different distribution and amount of the MPD monomers kept on the PES layer. As discussed in the previous section, the porosity and pore size of the PVDF-PES membranes tends to be smaller when increasing the concentration of PES, and the top structure becomes more uniform and denser. The poor uniformity of the surface structure shown in Figure 3(a) (PVDF + PES 13%) results in an unevenly distributed MPD aqueous solution over the PES layer, and an irregular polyamide structure is produced [Figure 4(a)]. Regarding the shape of the ridge-and-valley structures, when a large amount of MPD monomers kept in the large pores on the PES layer contact with the TMC organic solution, larger ridge structures are formed. On the contrary, less MPD yields less rough surface. Different from the observation in Figure 4(a)

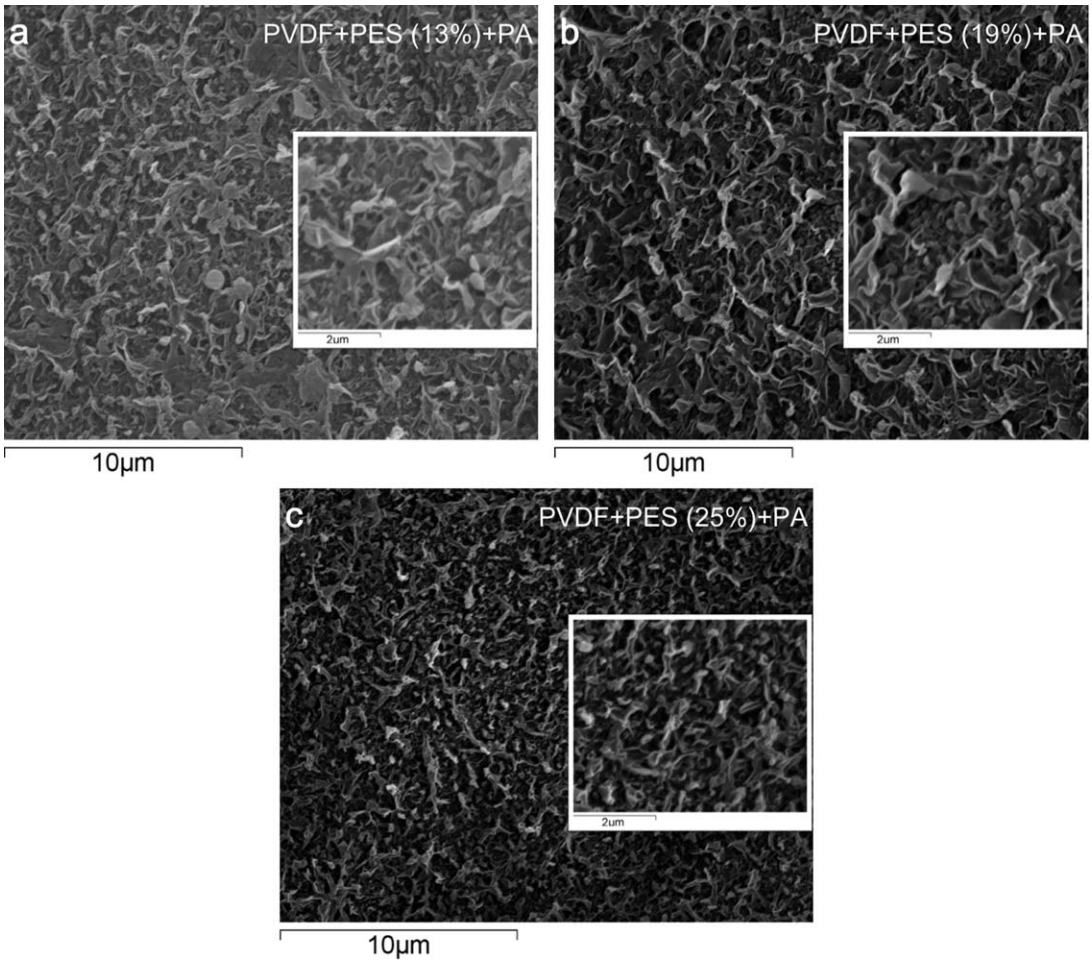

Figure 4. Surface morphologies of PVDF-PES-PA hollow fiber membranes with different concentrations of PES transitional layers. All of the membranes were supported by the same PVDF hollow fiber substrates and covered by the same PA top skins.

(PVDF + PES 13% + PA), the surface morphology of the membrane with a high concentration of the PES support layer [Figure 4(c)] has a relatively regular ridge-and-valley structure, which is due to the even distribution of the MPD on the uniform and dense PES surface. These polyamide structures can further influence the filtration performance of the composite hollow fiber membranes.

Filtration Performance of PVDF-PES-PA Hollow Fiber Membranes. Comparing the pure water permeability (PWP) before (Table I) and after (Figure 5) coating the polyamide layers, it is obvious that the polyamide layers cause a great transport resistance to water flux. For example, after coating the PVDF-PES (13%) hollow fiber membranes with polyamide, the PWP reduced from 1418 ± 27.1 to 22.25 ± 0.27 L m^{-2} h^{-1} bar^{-1}. The reduced percentage is as high as 98.4% of the initial PWP value. As the concentrations of the support PES layers increase to 28%, the reduced percentage of PWP before and after the polyamide coating decreases to 28.4%. These different flux losses for the PVDF-PES-PA membranes are caused by the different thickness and morphologies of polyamide formed in the PES layers. The polyamide formed inside and on the pores of

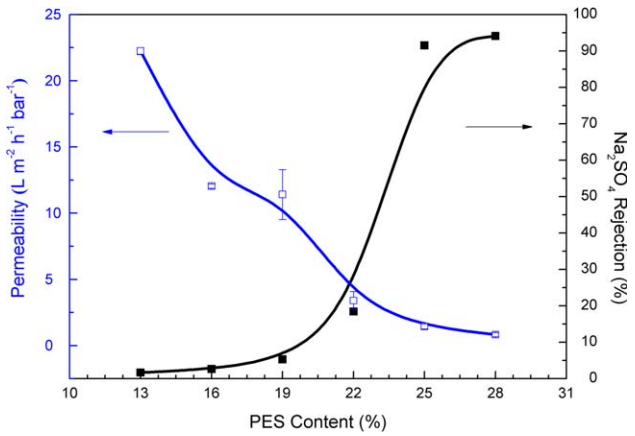

Figure 5. Filtration performance of PVDF-PES-PA hollow fiber membranes with different concentrations of PES transitional layers. All of the membranes were supported by the same PVDF hollow fiber substrates and covered by the same PA top skins. The permeability and salt rejections were tested by filtrating pure water and 1000 ppm Na_2SO_4 solutions, respectively. [Color figure can be viewed in the online issue, which is available at wileyonlinelibrary.com.]

the PES support layers is the main reason for the flux loss. As mentioned, the larger pores (e.g., PVDF-PES 13%) retain more MPD monomers, and a thicker polyamide layer or bigger ridge is formed on the pores. In this case, a higher transport resistance is generated and the reduced percentage of the PWP is larger. On the contrary, smaller pores lead to smaller ridges and a thinner polyamide layer, which yields less flux loss.

The retentions of the membranes are determined mainly by the degree of crosslinking and the uniformity of the polyamide layers. As shown in Figure 5, the retention of Na_2SO_4 is increased from 1.7 to 94.1% when the concentration of the PES layer varies from 13 to 28%. These changes in salt rejections are probably related to the different mean pore size of the supporting PVDF-PES membranes. The membranes coated by 16, 19, and 22% of the PES layers have a mean pore size of 15.5 nm, 15.2 nm, and 14.4 nm, respectively (Table II). The thin and weak polyamide layers formed in and on these large pores of the PVDF-PES membranes cannot stand for the high operational pressure, and breakage is formed in the polyamide layers. Due to this reason, the salt rejections of these PVDF-PES-PA membranes are very low (<20%). When increasing the concentration of the PES layer to 25%, the mean pore size of the PVDF-PES membrane reduces to 11.9 nm, which is significantly smaller than the one of the membrane with 22% of PES (Table II). This smaller pore size assures the uniformity and integrity of the polyamide layer under the high operational pressure. Due to this reason, the salt rejection sharply increases to 91.5%. The transitional filtration performance indicates that the additional polyamide coating process can further adjust the performance of the hollow fiber membranes from UF-like membranes to NF-like membranes. The tunable filtration performance can be simply achieved by changing the properties of the PES support layers.

CONCLUSIONS

An intensified production process has been developed to produce a new tailored hollow fiber membrane with tunable filtration performance, high mechanical strength and a great surface area per volume ratio. This intensified process combines the approaches of TIPS, NIPS, and IP in a single procedure. The PVDF hollow fiber membranes made by a TIPS method serve as porous and rigid supporting substrates. The PES layers produced by NIPS and the polyamide top skins made by IP are coated one after another. After coating the PES layers, the hollow fiber membranes can reject the dextran with a molecular weight of 20 kDa. As the concentration of the PES layer increases from 13% to 28%, the mean pore size of the PVDF-PES membrane decreases from 15.5 nm to 7.1 nm, and the tensile strength at break increases from 11.6 MPa to 17.3 MPa. These structural changes lead to a greatly reduced PWP. The initial PVDF MF hollow fiber membranes (150 nm of the mean pore size) cannot reject the organic solute with M_w of 300 kDa. After coating the PES layers, the MWCO of the PVDF-PES membranes is around 200 kDa and the mean pore size is reduced to around 10 nm that fits the category of ultrafiltration. By further adding polyamide layers, the final membranes have salt rejections up to 94.1% (28% of PES). All these results suggest that this intensified production process is capable to produce a hollow fiber membrane with tunable filtration performance from microfiltration-like to nanofiltration-like, while the great surface area per volume ratio is retained and the mechanical strength is enhanced.

REFERENCES

1. Stankiewicz, A. *Chem. Eng. Process* **2003**, *42*, 137.
2. Van der Bruggen, B.; Curcio, E.; Drioli, E. *J. Environ. Manage.* **2004**, *73*, 267.
3. Cui, Z.; Hassankiadeh, N. T.; Lee, S. Y.; Lee, J. M.; Woo, K. T.; Sanguineti, A.; Arcella, V.; Lee, Y. M.; Drioli, E. *J. Membr. Sci.* **2013**, *444*, 223.
4. Tsai, H.; Kuo, C.; Lin, J.; Wang, D.; Deratani, A.; Pochat-Bohatier, C.; Lee, K.; Lai, J. *J. Membr. Sci.* **2006**, *278*, 390.
5. Pendergast, M. M.; Hoek, E. M. *Energy Environ. Sci.* **2011**, *4*, 1946.
6. Irving Moch, J. *Kirk-Othmer Encyclopedia Chem. Technol.* **2005**, *16*, 1.
7. Wang, K. Y.; Chung, T.-S.; Gryta, M. *Chem. Eng. Sci.* **2008**, *63*, 2587.
8. Soltanieh, M.; Gill, W. N. *Desalination* **1984**, *49*, 57.
9. Chung, T.-S.; Qin, J.-J.; Gu, J. *Chem. Eng. Sci.* **2000**, *55*, 1077.
10. Yang, X.; Wang, R.; Fane, A. G.; Tang, C. Y.; Wenten, I. G. *Desalin. Water Treat.* **2013**, *51*, 3604.
11. Van de Witte, P.; Dijkstra, P.; Van den Berg, J.; Feijen, J. *J. Membr. Sci.* **1996**, *117*, 1.
12. Fane, A. G.; Tang, C. Y.; Wang, R. In Treatise on Water Science; Wilderer, P., Ed.; Elsevier: Oxford, **2011**; Vol. 4, Chapter 4.11, p 301.
13. Zhang, R. X.; Vanneste, J.; Poelmans, L.; Sotto, A.; Wang, X. L.; Van der Bruggen, B. *J. Appl. Polym. Sci.* **2012**, *125*, 3755.
14. Lee, M.-S.; Yoon, J.-K.; Choi, S.-H.; Shin, Y.-C. U.S. Pat. 8,201,485, **2012**.
15. Cote, P. L.; Pedersen, S. K. W.O. Pat. 2,010,148,517, **2010**.
16. Lee, M.-S.; Choi, S.-H.; Villa, W. H.; Shin, Y.-C. C. E.P. Pat. 1,321,178, **2011**.
17. Van der Bruggen, B.; Schaep, J.; Wilms, D.; Vandecasteele, C. *J. Membr. Sci.* **1999**, *156*, 29.
18. Dubois, M.; Gilles, K. A.; Hamilton, J. K.; Rebers, P. t.; Smith, F. *Anal. Chem.* **1956**, *28*, 350.
19. Wang, X.-L.; Tsuru, T.; Nakao, S.-i.; Kimura, S. *J. Membr. Sci.* **1997**, *135*, 19.
20. Idris, A.; Mat Zain, N.; Noordin, M. *Desalination* **2007**, *207*, 324.
21. Singh, S.; Khulbe, K.; Matsuura, T.; Ramamurthy, P. *J. Membr. Sci.* **1998**, *142*, 111.
22. Peeva, P. D.; Million, N.; Ulbricht, M. *J. Membr. Sci.* **2012**, *390*, 99.

23. Sarbolouki, M. *Sep. Sci. Technol.* **1982**, *17*, 381.

24. Kools, W. F. C. In Membrane Formation by Phase Inversion in Multicomponent Polymer Systems: Mechanisms and Morphologies; PhD Thesis; Department of Chemical Engineering: University of Twente, **1998**.

25. Ghosh, A. K.; Hoek, E. *J. Membr. Sci.* **2009**, *336*, 140.

26. Tang, C. Y.; Kwon, Y.-N.; Leckie, J. O. *J. Membr. Sci.* **2007**, *287*, 146.

27. Kwak, S. Y.; Jung, S. G.; Yoon, Y. S.; Ihm, D. W. *J. Polym. Sci. Part B: Polym. Phys.* **1999**, *37*, 1429.

28. Morgan, P. W.; Kwolek, S. L. *J. Polym. Sci.* **1959**, *40*, 299.

29. Freger, V. *Langmuir* **2003**, *19*, 4791.